ACS APPLIED MATERIALS & INTERFACES

www.acsami.org

Research Article

Reversible Hydrogen Storage in Metal-Decorated Honeycomb Borophene Oxide

Parsa Habibi, Thijs J. H. Vlugt, Poulumi Dey, and Othonas A. Moultos*

Cite This: *ACS Appl. Mater. Interfaces* 2021, 13, 43233−43240

Read Online

ACCESS | Metrics & More | Article Recommendations | Supporting Information

ABSTRACT: Two-dimensional (2D) boron-based materials are receiving much attention as H_2 storage media due to the low atomic mass of boron and the stability of decorating alkali metals on the surface, which enhance interactions with H_2. This work investigates the suitability of Li, Na, and K decorations on 2D honeycomb borophene oxide (B_2O) for H_2 storage, using dispersion corrected density functional theory (DFT-D2). A high theoretical gravimetric density of 8.3 wt % H_2 is achieved for the Li-decorated B_2O structure. At saturation, each Li binds to two H_2 with an average binding energy of −0.24 eV/H_2. Born−Oppenheimer molecular dynamics simulations at temperatures of 100, 300, and 500 K demonstrate the stability of the Li-decorated structure and the H_2 desorption behavior at different temperatures. Our findings indicate that Li-decorated 2D B_2O is a promising material for reversible H_2 storage and recommend experimental investigation of 2D B_2O as a potential H_2 storage medium.

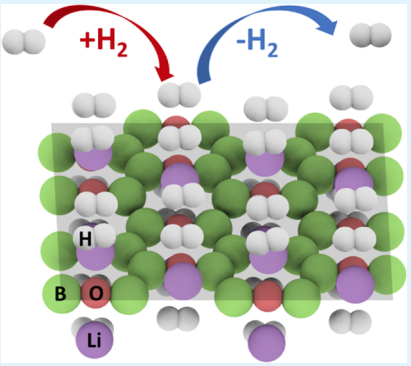

KEYWORDS: *hydrogen, hydrogen storage, borophene oxide, physisorption, hydrogen binding energy, density functional theory, Born−Oppenheimer molecular dynamics, metal decoration*

1. INTRODUCTION

Conventional methods of hydrogen (H_2) storage, which include highly pressurized chambers or cryogenic cooling, are energy-intensive, lead to boil-off losses, and may require thick storage walls.[1,2] For these reasons, chemisorption and physisorption-based H_2 storage systems have emerged as an alternative.[1,3,4] Chemisorption-based H_2 storage in hydrides, such as MgH_2, leads to high capacities but slow adsorption/desorption kinetics due to strong covalent interactions with H atoms.[4−7] Physisorption-based H_2 storage, for example in metal−organic frameworks (MOFs), leads to faster adsorption/desorption kinetics but lower H_2 capacities due to the weak (van der Waals) interactions of the porous framework with H_2.[8−11] Among physisorption-based H_2 storage materials, two-dimensional (2D) structures exhibit great potential in reaching high H_2 capacities due to their large surface to volume ratios.[12−14] To achieve reversible H_2 storage, the binding of H_2 on the 2D substrate generally needs to be enhanced. Several adjustments have been proposed to enhance the binding of H_2 with 2D substrates.[13,15−19] Examples of such adjustments include external charge modulation,[16,17] and introduction of decorating atoms (mainly metals such as Li), which enhance interactions by polarizing H_2.[13,18,19] 2D boron sheets (borophene), which have been recently synthesized,[20−22] have shown a favorable affinity for different metal-decorating atoms, in contrast to graphene, in which clustering of metal atoms can occur.[23,24] Using a variety of metal decorations, such as Li,[18,19,23] Na,[25] Ca,[26] and Ti[27] on different borophene polymorphs, impressive H_2 gravimetric densities have been obtained ranging from 6 to 15 wt %, exceeding the US department of energy (DOE) requirement for onboard storage of 6.5 wt % H_2.[28]

Experimental and theoretical studies on borophene have indicated that borophene is prone to oxidation when exposed to air.[20,29−31] For this reason, the protection of borophene polymorphs from air can be crucial for applications such as H_2 storage.[31] Although uncontrolled oxidation is undesirable, one can intentionally use the oxidation process to produce structures that are more chemically stable.[32,33] For this reason, researchers have been actively looking into a variety of 2D boron oxide structures.[33,34] Inspired by the recent synthesis of honeycomb borophene on an Al substrate,[21,32] a 2D honeycomb borophene oxide (B_2O) structure has been theoretically proposed.[32] Phonon dispersion and ab initio molecular dynamics simulations have shown that the 2D honeycomb B_2O structure is stable at temperatures up to 1000 K.[32] 2D honeycomb B_2O has a high capacity for Li/Na functionalization, thereby being a promising anodic material.[35] In particular, B_2O has been shown to have one of the highest capacities for Li storage.[35] The high affinity of 2D B_2O to

Received: May 27, 2021
Accepted: August 18, 2021
Published: August 30, 2021

https://doi.org/10.1021/acsami.1c09865
ACS Appl. Mater. Interfaces 2021, 13, 43233−43240

metal-decorating atoms, with its high stability hints at the suitability of this material for H_2 storage applications. Similar to other 2D boron-based structures, such as borophene,[36] 2D boron oxides can form different structural polymorphs.[33,34,37] Honeycomb B_2O has lower formation energy compared to other 2D allotropes such as B_4O, B_5O, B_6O, B_7O, and B_8O indicating its stability.[32,33] Other 2D polymorphs of boron oxide such as the recently reported B_2O_3[37] may also be suitable for H_2 storage applications, however, the study of these materials is beyond the scope of this work.

In this work, the use of 2D B_2O as an efficient H_2 storage material is investigated using first-principles calculations. Three different alkali metals (i.e., Li, Na, and K) are considered for enhancing the interactions of 2D B_2O with H_2. The addition of these metal-decorating atoms is found to be favorable as evident by negative adsorption energies. All three metal atom types increase the binding energy of H_2 compared to the pristine structure and result in binding energies suitable for reversible H_2 storage. Our density functional theory (DFT) calculations with the Li-decorated 2D B_2O structure clearly show that a notable gravimetric density of 8.3 wt % H_2 can be achieved. By performing Born−Oppenheimer molecular dynamics (BOMD) simulations we show that the Li-decorated structure is stable at 100, 300, and 500 K. Finally, we used semi-empirical calculations to show that under adsorption conditions of 298 K and 30 atm and desorption conditions of 373 K and 3 atm, a practical gravimetric density of 5.2 wt % H_2 can be attained. Our findings strongly recommend further experimental investigation of 2D honeycomb B_2O as a potential H_2 storage medium.

2. COMPUTATIONAL DETAILS

2.1. Density Functional Theory. DFT calculations are carried out using plane-wave basis sets, as implemented in the Vienna ab initio simulation package (VASP 5.3.5).[38,39] The projected augmented wave method (PAW) is used and the generalized gradient approximation (GGA) is applied with the Perdew−Burke−Ernzerhof (PBE) exchange-correlation functional.[40] Van der Waals forces are accounted for using a dispersion corrected framework (DFT-D2).[41] This approach is commonly used in other studies of H_2 storage on 2D metal-decorated substrates.[13,15,18,27,42] An inter-layer separation of more than 30 Å is used to prohibit inter-layer interactions.[19] Nevertheless, a smaller inter-layer spacing may also be applicable.[15,18,42] The cut-off energy is set to 700 eV for the plane-wave basis set and a Γ-centered Monkhorst−Pack k-point mesh of 3 × 9 × 1 is used for the structural relaxations and binding energy calculations. The energy convergence criteria for the self-consistent electronic loop is set to 10^{-6} eV. All lattice parameters and atomic positions are relaxed until the residual forces acting on each atom are below 1 meV/Å. Gaussian smearing with a σ of 0.02 eV is used for Brillouin-zone integration. A 2 × 2 conventional unit cell of borophene oxide, containing 16 B atoms and 8 O atoms, is used for the DFT simulations. The H_2 adsorption energies are calculated from[18,43−46]

$$E_b = (E_{S+qH_2} - E_S - qE_{H_2})/q \quad (1)$$

where E_b is the average binding energy of H_2 with the 2D substrate, E_{S+qH_2} and E_S are the energies of the substrate with and without H_2 molecules, E_{H_2} is the energy of a H_2 molecule in a vacuum, and q is the number of H_2 molecules. All energies in eq 1 are computed using DFT. For simulations in which the 2D structure is functionalized with metals atoms, the average H_2 binding energy is calculated using[18,43−46]

$$E_b = (E_{S+M+qH_2} - E_{S+M} - qE_{H_2})/q \quad (2)$$

where E_{S+M+qH_2} and E_{S+M} represent the energy of the 2D metal-decorated substrate with and without H_2, respectively. The single H_2 removal energy, E_r, is calculated according to[47]

$$E_r = E_{S+M+qH_2} - E_{S+M+(q-1)H_2} - E_{H_2} \quad (3)$$

where E_{S+M+qH_2} and $E_{S+M+(q-1)H_2}$ represent the energies of a 2D metal-decorated substrate containing q and $(q-1)$ H_2 molecules, respectively. In the case of metal-decorated 2D B_2O there is an intrinsic dipole in the direction normal to the 2D plane. For this reason, calculations are carried out to examine if there is a need for dipole corrections in this system. It is found that for single-metal (Li, Na, and K)-decorated B_2O dipole corrections change the total energies by less than 0.02% and the metal adsorption energies on B_2O by less than 2.5% (most different for K-decorated and the least for Li-decorated B_2O). As the results do not show considerable change, dipole corrections were not accounted for the rest of the computations.

2.2. Born−Oppenheimer Molecular Dynamics (BOMD). To investigate the finite temperature stability of the structure, BOMD simulations are carried out using VASP. To create the BOMD simulation box, the DFT supercell is multiplied by a factor of 2 along its smallest side, thereby creating a 2 × 4 supercell. The stability of the H_2-saturated and Li-decorated B_2O structure is examined at three different temperatures (i.e., 100, 300, and 500 K) using the Nosé−Hoover thermostat.[48,49] These simulations are performed in the canonical ensemble (NVT) and include only the Γ-point. Alternatively, the NPT ensemble can be used for the simulations. As the number of H_2 molecules is relatively small (32 in total), large pressure fluctuations are expected upon adsorption/desorption of H_2. Due to this when using the NPT ensemble caution must be taken to adjust only the volume normal to the 2D plane, to avoid creating artifacts (e.g., artificial wrinkles) on the 2D structure. For this reason, the NVT ensemble is chosen. The same cut-off energy and smearing as in the DFT calculations are used. The "normal" precision mode is used for the BOMD simulations and the "accurate" precision mode is used for the DFT simulations. The BOMD simulations are carried out with a time-step of 1 fs, for a total time of 10 ps. The Verlet algorithm is used for integrating the equations of motion.[50] The variation of free energy (as defined by Kresse et al.[38]) as a function of simulation time is shown in Figure S1. In all BOMD simulations, an equilibration period of 5 ps is initially performed. Production runs of 5 ps are used for sampling the property of interest. VESTA is used for all atomic visualizations.[51]

3. RESULTS AND DISCUSSION

3.1. Pristine B_2O Structure. The planar 2D structure of honeycomb B_2O is shown in Figure 1. Our results indicate that the relaxed lattice constants for the conventional unit cell are 2.76 and 7.37 Å, while the lattice constant for the primitive cell is 3.93 Å (both sides are equal). The optimal B−O and B−B bond lengths in our simulations are computed to be 1.34 and 1.71 Å, respectively. These results agree well with other DFT

https://doi.org/10.1021/acsami.1c09865
ACS Appl. Mater. Interfaces 2021, 13, 43233−43240

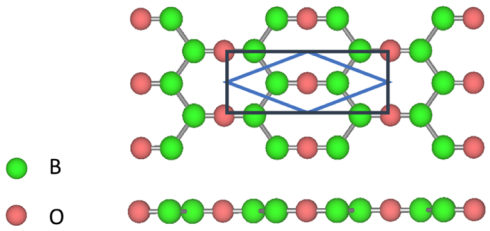

Figure 1. Top and side view of the 2D honeycomb borophene oxide structure. The lattice constant for the primitive cell (shown with blue lines) is 3.93 Å, and the lattice constants for the conventional cell (shown with black lines) are 2.76, and 7.37 Å.

results from the literature.[32,33] A single H_2 molecule is then added to the system to compute the binding to the 2D B_2O structure. According to eq 1, a single H_2 adsorbs with a binding energy of −0.10 eV/H_2 to the 2D B_2O structure. Figure S2 shows different initial configurations that are probed and the final relaxed configuration of H_2 on 2D B_2O. All of the different initial configurations converged into the same final configuration after relaxing all atomic positions and the structural parameters. Although the binding energy of H_2 with the pristine borophene oxide structure is higher than that of striped borophene (c.a. −0.05 eV/H_2),[18] this binding energy is not adequate for reversible storage of H_2.[52−55] This illustrates the necessity for the addition of metal-decorating atoms.

3.2. Metal Decoration. Three different alkali metal-decorating atoms have been probed, i.e., Li, Na, and K. These alkali metal atoms have shown to be particularly adept at enhancing the interaction with H_2, for other 2D structures such as striped borophene,[18] boron phosphide,[15] and boron hydride.[42] Other metal decorations such as Ca and Ti have also shown to be suitable for H_2 storage applications on 2D borophene structures,[26,27] but examining the applicability of these or other metal atoms as dopants on 2D B_2O for H_2 storage is beyond the scope of this work. Before assessing the influence of the decorating atoms on the binding of H_2, the adsorption energy of these metal atoms is calculated on the B_2O surface according to[35]

$$E_{ads} = E_{S+M} - E_S - E_{M,C} \quad (4)$$

where E_{ads}, E_{S+M}, $E_{M,C}$, and E_S are the energy of adsorption, the energy of the substrate plus the metal atom, the cohesive energy of the bulk crystalline metal, and the energy of the substrate, respectively. A negative adsorption energy signifies the favorable adsorption of the metal atom on the 2D substrate and a positive energy means that the metal atoms would preferentially cluster together.[15] The values of E_{ads} are −1.00, −0.71, and −1.11 eV for a single Li, Na, and K-decorated 2D B_2O structure, respectively. All three metal-decorating atoms i.e., Li, Na, and K prefer the hollow position in the ring of honeycomb B_2O (see Figure 2a for Li) and are situated at a distance of 1.40, 2.02, and 2.41 Å, respectively (see Figure S3 for different configurations). The charge density difference plot of a Li-decorated system is shown in Figure 2b. This charge density difference plot is calculated using[15]

$$\Delta\rho = \rho_{S+M} - \rho_S - \rho_M \quad (5)$$

where $\Delta\rho$, ρ_S, ρ_M, and ρ_{S+M} represent the charge density difference, charge density of the substrate, the metal atom, and the combined structure, respectively.

In Figure 2b, it can be seen that the addition of the Li atom to the B_2O substrate leads to the formation of a charge depleted region on top of Li (blue region as indicated in Figure 2b), while there is an enhancement of the charge density for the boron and oxygen atoms in the vicinity of Li (yellow region in Figure 2b). Bader charge analysis carried out on Li-, Na-, and K-decorated B_2O (see Table S1) illustrates the loss of electronic charge by decorating the 2D substrate with alkali metals. A H_2 molecule that is added to this system interacts with the metal atom and is adsorbed in the charge depleted region as shown in Figure 2c. Figure S4 shows different configurations that are considered for H_2 adsorption on Li, Na, and K-decorated 2D B_2O. For the Li-decorated structure, H_2 preferentially adsorbs on top of the O-atom, in the vicinity (top edge) of the Li atom (as seen in Figure 2c). The favourability of this position is attributed to H_2 maximizing its attractive interaction with the Li atom (and its periodic image) and the 2D B_2O sheet. Similarly, for the Na and K-decorated system (see Figure S4) this site is found to be the most favorable, although the exact positioning of H_2 differs due to the different atomic sizes of Na and K compared to Li. The results for the adsorption of a single H_2 indicate a binding energy of −0.34 eV/H_2 in the case of the Li-decorated structure, and a binding energy of −0.25 and −0.28 eV/H_2 for Na- and K-decorated structures, respectively. These calculations show that all of the alkali metal (i.e., Li, Na, K)-decorated B_2O structures have resulted in an interaction energy in the range suitable for reversible H_2 storage (above −0.10 and below −0.60 eV/H_2).[52−55] For further calculations of the H_2 gravimetric density, the Li-decorated structure is investigated in more detail because of its higher interaction

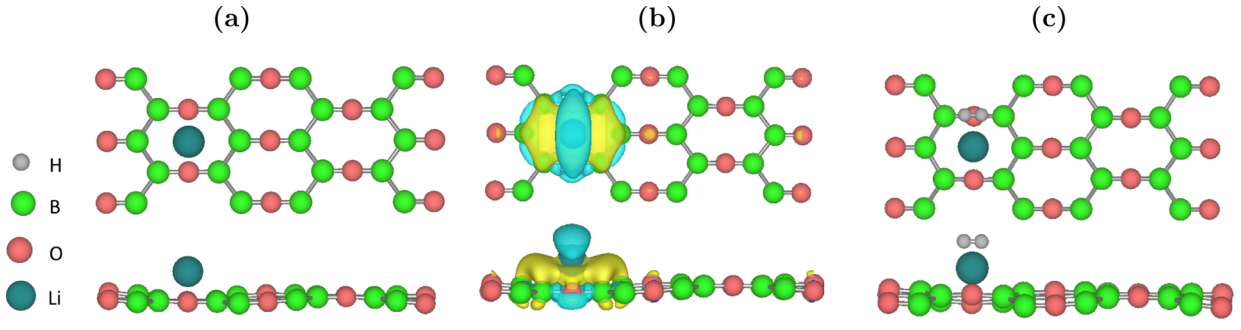

Figure 2. Top and side views of (a) a single Li-decorated 2D honeycomb B_2O structure, (b) the charge density difference of the Li-decorated structure, the isosurface value is set to 0.0015 e/Å^3 (blue areas represent charge density depletion, while yellow areas represent gain), and (c) an adsorbed H_2 on the Li-decorated structure, with the H_2 orientation parallel to the B−O−B bond.

https://doi.org/10.1021/acsami.1c09865
ACS Appl. Mater. Interfaces 2021, 13, 43233−43240

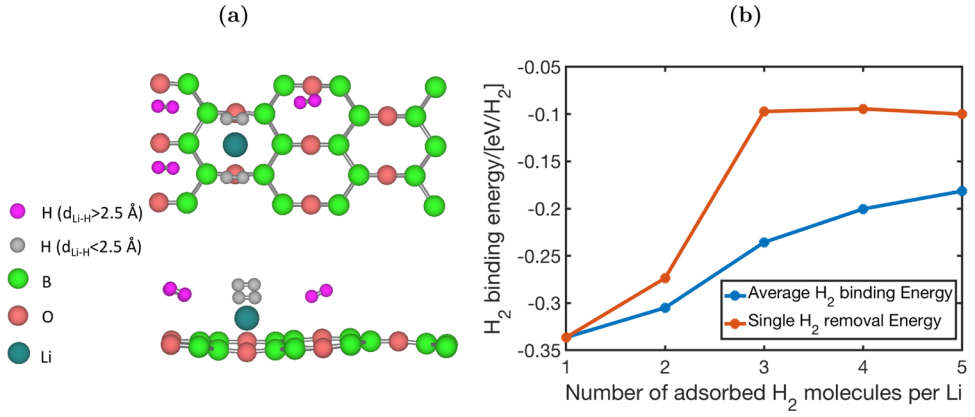

Figure 3. (a) Top and side views of a structure containing 5 H_2 surrounding one Li atom. Two H_2 are within a 2.5 Å radius from Li (shown in gray), while the other three are further away due to repulsive forces (shown in pink). (b) The variation of the average H_2 binding energy (E_b) and H_2 removal energy (E_r) as a function of the number of adsorbed H_2 molecules per Li. The lines connecting the points are used to guide the eye.

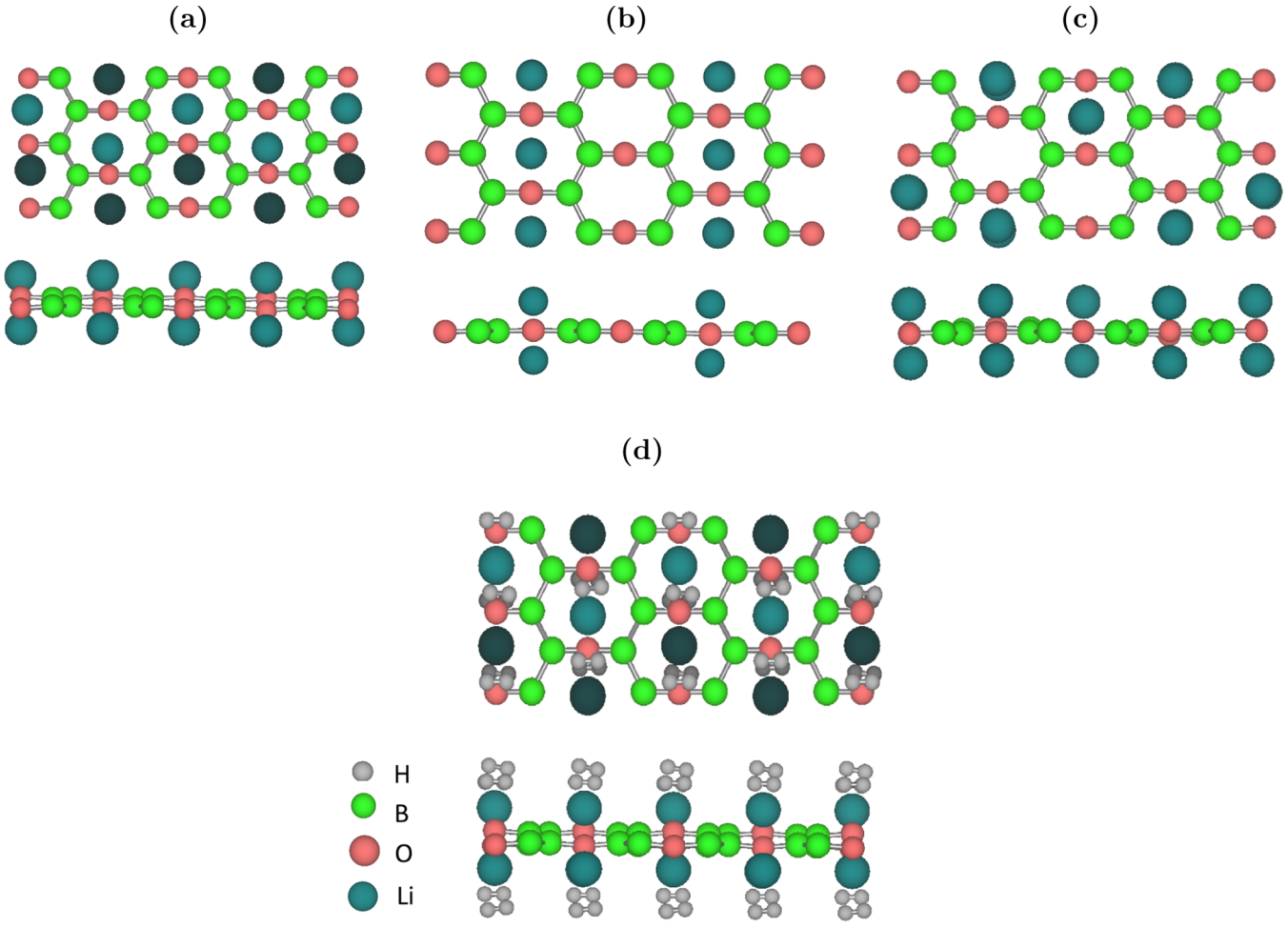

Figure 4. (a–c) Different configurations of the half-covered Li structures shown from the top and the side. (d) Top and side view of H_2 adsorption in structure (a). Each Li atom can successfully bind to two H_2 leading to a gravimetric density of 8.3 wt % H_2. In the top view, the Li and H atoms that are at the bottom are given a darker shade for better readability of the figure.

energy with H_2 and the lower atomic mass of Li compared to Na and K.

3.3. H_2 Gravimetric Density. To test the suitability of Li-decorated honeycomb B_2O for H_2 storage, it is important to estimate the maximum theoretical gravimetric density of H_2 in this structure. For this, both the number of H_2 and Li atoms need to be systematically increased. Before increasing the number of Li atoms it is useful to obtain an estimate of the number of H_2 molecules one Li atom can bind to, and how the average binding energy between H_2 and the metal-decorated structure changes with the addition of H_2.

To visualize how H_2 molecules disperse around the Li atom, a structure containing five H_2 surrounding one Li atom is shown in Figure 3a. Out of the five H_2 that are shown in this

https://doi.org/10.1021/acsami.1c09865
ACS Appl. Mater. Interfaces 2021, 13, 43233−43240

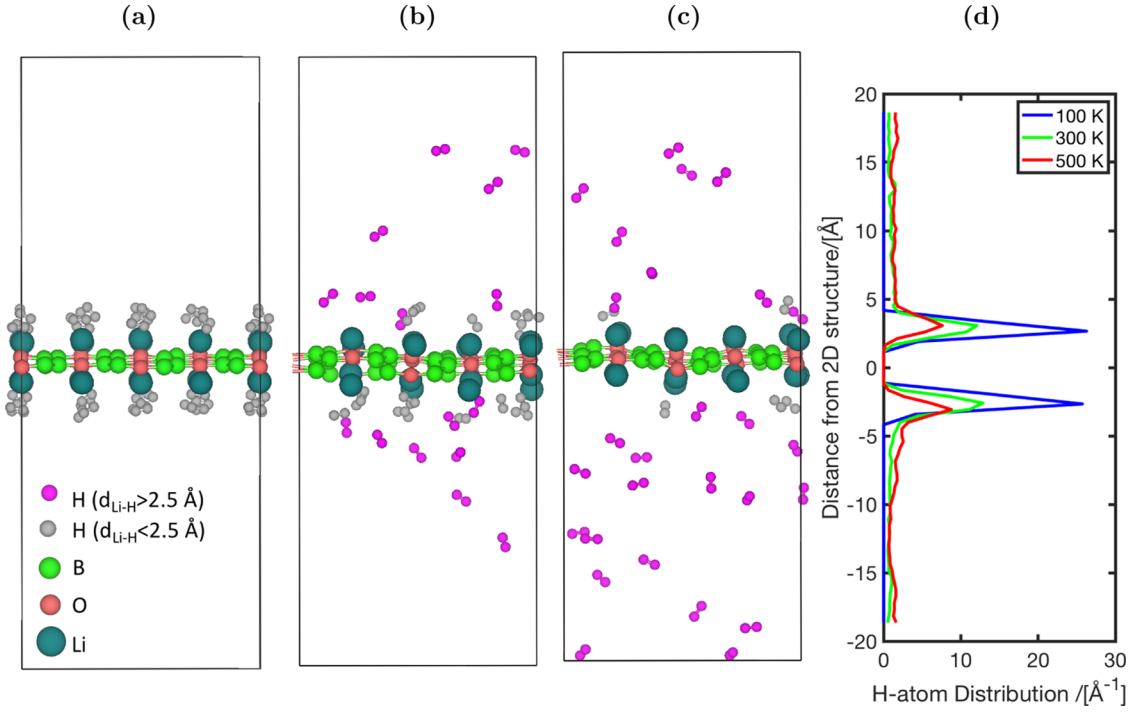

Figure 5. BOMD simulation snapshots of the Li-decorated B_2O structure at three different temperatures of (a) 100 K, (b) 300 K, and (c) 500 K. H_2 molecules that are at a distance exceeding 2.5 Å from the closest neighboring Li atom are colored in purple while the ones within this range are colored in gray. The average H-atom distribution calculated over the last 5 ps of the BOMD simulations as a function of the distance perpendicular to the surface (d).

figure, two H_2 have a distance lower than 2.5 Å from Li, while the other three are positioned at a distance of more than 2.5 Å from the Li atom. In Figure 3b the average binding energy per H_2 and the H_2 removal energy is shown as a function of the number of H_2 molecules per Li atom. In a single Li-decorated system, when the number of H_2 molecules is increased from 2 to 3, a large decrease in the magnitude of the H_2 removal energy is observed from −0.27 eV/H_2 to around −0.10 eV/H_2. Considering that −0.10 eV/H_2 is approximately the interaction energy of H_2 with borophene oxide in the absence of Li, it can be concluded that the 3rd to 5th H_2 molecules interact very weakly with Li. Based on the findings shown in Figure 3, it is evident that each Li atom can optimally interact with two H_2 molecules, with an average binding energy of −0.30 eV/H_2. Considering that H_2 preferentially binds to the top sides of the Li atom, parallel to the B−O−B bond, it is not suitable to fully cover the structure with Li atoms (i.e., two Li atoms in each hexagonal hole, one at the top and the other at the bottom). Overloading the structure with Li atoms will reduce the number of H_2 that can be adsorbed per Li atom, and thus, lead to a lower H_2 gravimetric density. For this reason, a "half-covered" structure of Li atoms (i.e., a structure containing half as many Li atoms as a fully covered structure) is deemed optimal.

Different half-covered Li configurations are shown in Figure 4a−c. From the three structures shown, structure (a) is the most energetically stable, while structure (b) has the highest energy (with a relative difference of 1.5% compared to the energy of structure (a)). Structure (c) has a relative energy difference of only 0.3% with respect to structure (a). Considering that structure (a) is the most energetically stable configuration, it is used for further calculations of H_2 adsorption. The addition of two H_2 on the top side of each Li atom (as depicted in Figure 4d) resulted in an average binding energy of −0.24 eV/H_2. The weakest H_2 binding energy (H_2 removal energy from the fully H_2 saturated structure shown in Figure 4d) is calculated to be −0.21 eV/H_2, while the strongest H_2 binding energy (H_2 binding energy for the first H_2 added to the structure shown in Figure 4a) is −0.27 eV/H_2. Each H_2 in this structure is located at a distance lower than 2 Å from a Li atom. The gravimetric density (GD) of H_2 can be calculated using[18]

$$\mathrm{GD} = \frac{qM_{H_2}}{qM_{H_2} + nM_B + lM_O + kM_m} \quad (6)$$

where q, n, l, and k represent the number of H_2 molecules, B, O, and metal-decorating atoms in the simulation box, respectively, while M denotes their respective molar masses. Using eq 6, the H_2 gravimetric density of this structure equals 8.3 wt %, which exceeds the 6.5 wt % target set by the DOE.[28]

3.4. Finite Temperature Stability. To further check the stability and desorption of H_2 at finite temperatures, BOMD simulations are carried out at target temperatures of 100, 300, and 500 K. The results are shown in Figure 5. Figure 5a−c depicts the BOMD snapshots after 10 ps. From these sub-figures, it can be seen that at 100 K, all of the H_2 molecules are bound to the Li-decorated B_2O structure, at 300 K 50%, and at 500 K ∼85% of the H_2 molecules are at distances larger than 2.5 Å from the Li atom. To obtain a more quantitative measure of the desorption process, the H-atom distribution in the simulation box is plotted as a function of the distance perpendicular to the 2D surface. The distribution plot is normalized such that the area under the curve equates to the number of H atoms in the simulation. Figure 5d shows two peaks, both at a distance of ∼3 Å away from the 2D structure, which corresponds to the perpendicular distance of the H_2

https://doi.org/10.1021/acsami.1c09865
ACS Appl. Mater. Interfaces 2021, 13, 43233−43240

adsorption sites (above and below) from the 2D structure. The adsorption peak gradually decreases with the increase in the temperature, as H_2 molecules begin to distribute evenly in the simulation box. The BOMD simulations also demonstrate that even at 500 K, no clustering of Li atoms is observed in the 10 ps simulation time frame, and the metal-decorated structure is found to be stable. This confirms the favorable Li adsorption energy as discussed in Section 3.2. No chemical reactions have occurred between H_2 molecules and the 2D substrate, so the structure does not undergo irreversible changes and H_2 molecules can be released without having to overcome a significant energy barrier (covalent bond formation/breaking). Therefore, the findings from the BOMD simulations indicate the stability of Li-decorated B_2O for H_2 storage in the temperature range of 100−500 K.

3.5. Adsorption and Desorption Conditions. In the BOMD simulations, the pressure is not controlled and can vary considerably at different temperatures. In this section, semi-empirical calculations are used to estimate the practical H_2 storage capacity at finite temperatures and pressures. The occupation number (F), which represents the expected number of H_2 molecules that can be adsorbed on the structure, can be calculated using[56]

$$F = \frac{\sum_{n=0}^{N_{max}} n g_n \exp\left[\frac{n(\mu - E_b)}{k_B T}\right]}{\sum_{n=0}^{N_{max}} g_n \exp\left[\frac{n(\mu - E_b)}{k_B T}\right]} \quad (7)$$

where N_{max} is the maximum number of H_2 molecules that can be adsorbed, g_n is the degeneracy of a state containing n H_2, and E_b, T, k_B, and μ represent the average H_2 binding energy (function of n), temperature, Boltzmann constant, and chemical potential of H_2 in the gas phase, respectively. To simplify the expression, it is assumed that each adsorption site on the structure is independent of its neighboring sites. In this case, the situation simplifies to finding the occupation number of a single site (f), on which at most a single H_2 can be adsorbed. In this case, the degeneracy of the occupied and unoccupied state are both 1 and the single site occupation number equates to[13,47,54,57]

$$f = \frac{1}{1 + \exp\left[\frac{-(\mu - E_b)}{k_B T}\right]} \quad (8)$$

where the chemical potential of H_2 in the gas phase μ is a function of temperature and pressure. The total occupation number F and the single site occupation number f are related by $F = M_{sites} f$, in which M_{sites} refers to the total number of H_2 adsorption sites on the structure.[54] The chemical potential μ in our calculations is obtained using the empirical relation[47,54,57,58]

$$\mu(T, P)/[\text{eV}] = \mu_{ideal}(T, P) + 0.00015(T - 186.5) + 0.00065\left[(\log_{10}\frac{P}{P_0} - 0.5)^2 - 0.25\right] \quad (9)$$

where the temperature (T) is in the unit of K, pressure (P) is in the unit of atm, and the reference pressure (P_0) is 1 atm. μ_{ideal} is the ideal chemical potential and is calculated using[56]

$$\mu_{ideal}(T, P) = -k_B T \ln\left[\left(\frac{2\pi m_{H_2} k_B T}{h^2}\right)^{3/2} \frac{k_B T}{P}\right] \quad (10)$$

where h is Planck's constant and m_{H_2} is the mass of a single H_2 molecule. In our calculations, adsorption takes place at a temperature of 298 K and a pressure of 30 atm, while desorption occurs at 373 K and 3 atm. These adsorption/desorption conditions are often used in the literature for calculating the practical gravimetric density.[13,42,47,54,57] Under these conditions, the chemical potential (as calculated by eq 9) and the ideal chemical potential are similar in value.[57] Under adsorption conditions, the ideal chemical potential is −0.21 eV, while a value of −0.22 eV is obtained using eq 9. Under desorption conditions, the ideal chemical potential gives a value of −0.36 eV, while μ is obtained as −0.38 eV using eq 9.[57] Calculating f under the adsorption conditions yields a value of 0.64, while under the desorption conditions f becomes 0.01. This gives a practical gravimetric density of around 5.2 wt % H_2 for the Li-decorated B_2O under these capture/release conditions. Lowering the adsorption temperature and/or increasing the adsorption pressure can lead to higher gravimetric capacities. These findings indicate that the Li-decorated B_2O structure can be used for reversible H_2 storage, under near-ambient conditions. To obtain the optimal release/capture conditions and more accurate calculations of H_2 capacity at various temperatures and pressures, further simulations are encouraged.

4. CONCLUSIONS

The capability of 2D honeycomb borophene oxide for H_2 storage applications is assessed using DFT and BOMD simulations. This 2D structure has a favorable affinity with alkali metal atoms such as Li, Na, and K, as indicated by the negative adsorption energy of these metals. These alkali metal-decorated B_2O structures have enhanced H_2 binding energies with respect to the pristine B_2O structure. In particular, the Li-decorated structure reaches a gravimetric density of 8.3 wt % H_2 with an average binding energy of −0.24 eV/H_2, which exceeds the gravimetric density requirement set by DOE for onboard H_2 storage applications.[28] BOMD simulations at 100, 300, and 500 K and calculations of the occupation number show both the stability and reversible binding of H_2 on the Li-decorated borophene oxide structure. Our simulations strongly encourage experiments on borophene oxide and further simulations to accurately find the H_2 capacity at various pressures and temperatures.

■ ASSOCIATED CONTENT

Supporting Information

The Supporting Information is available free of charge at https://pubs.acs.org/doi/10.1021/acsami.1c09865.

Free energy plots as a function of time during Born−Oppenheimer molecular dynamics simulations of H_2 saturated, Li-decorated 2D honeycomb B_2O; different configurations of a single Li, Na, and K atom on 2D B_2O and their respective energy differences; and Bader charge analysis of single Li, Na, and K-decorated 2D B_2O (PDF)

https://doi.org/10.1021/acsami.1c09865
ACS Appl. Mater. Interfaces 2021, 13, 43233−43240

AUTHOR INFORMATION

Corresponding Author

Othonas A. Moultos − *Engineering Thermodynamics, Process & Energy Department, Faculty of Mechanical, Maritime and Materials Engineering, Delft University of Technology, 2628 CB Delft, The Netherlands;* orcid.org/0000-0001-7477-9684; Email: O.moultos@tudelft.nl

Authors

Parsa Habibi − *Engineering Thermodynamics, Process & Energy Department, Faculty of Mechanical, Maritime and Materials Engineering, Delft University of Technology, 2628 CB Delft, The Netherlands*

Thijs J. H. Vlugt − *Engineering Thermodynamics, Process & Energy Department, Faculty of Mechanical, Maritime and Materials Engineering, Delft University of Technology, 2628 CB Delft, The Netherlands;* orcid.org/0000-0003-3059-8712

Poulumi Dey − *Department of Materials Science and Engineering, Faculty of Mechanical, Maritime and Materials Engineering, Delft University of Technology, 2628 CD Delft, The Netherlands*

Complete contact information is available at: https://pubs.acs.org/10.1021/acsami.1c09865

Notes

The authors declare no competing financial interest.

ACKNOWLEDGMENTS

This work was sponsored by NWO domain Science for the use of supercomputer facilities, with financial support from the Nederlandse Organisatie voor Wetenschappelijk Onderzoek (The Netherlands Organization for Scientific Research, NWO). T.J.H.V. acknowledges NWO-CW for a VICI grant.

REFERENCES

(1) Durbin, D.; Malardier-Jugroot, C. Review of Hydrogen Storage Techniques for on Board Vehicle Applications. *Int. J. Hydrogen Energy* **2013**, *38*, 14595−14617.

(2) Eberle, U.; Felderhoff, M.; Schueth, F. Chemical and Physical Solutions for Hydrogen Storage. *Angew. Chem., Int. Ed.* **2009**, *48*, 6608−6630.

(3) Jena, P. Materials for Hydrogen Storage: Past, Present, and Future. *J. Phys. Chem. Lett.* **2011**, *2*, 206−211.

(4) Schneemann, A.; White, J. L.; Kang, S.; Jeong, S.; Wan, L. F.; Cho, E. S.; Heo, T. W.; Prendergast, D.; Urban, J. J.; Wood, B. C.; Allendorf, M. D.; Stavila, V. Nanostructured Metal Hydrides for Hydrogen Storage. *Chem. Rev.* **2018**, *118*, 10775−10839.

(5) Er, S.; de Wijs, G. A.; Brocks, G. Tuning the Hydrogen Storage in Magnesium Alloys. *J. Phys. Chem. Lett.* **2010**, *1*, 1982−1986.

(6) Li, Q.; Qiu, S.; Wu, C.; Lau, K. T.; Sun, C.; Jia, B. Computational Investigation of MgH_2/Graphene Heterojunctions for Hydrogen Storage. *J. Phys. Chem. C* **2021**, *125*, 2357−2363.

(7) Wu, R.; Ren, Z.; Zhang, X.; Lu, Y.; Li, H.; Gao, M.; Pan, H.; Liu, Y. Nanosheet-like Lithium Borohydride Hydrate with 10 wt % Hydrogen Release at 70 °C as a Chemical Hydrogen Storage Candidate. *J. Phys. Chem. Lett.* **2019**, *10*, 1872−1877.

(8) Yang, S. J.; Jung, H.; Kim, T.; Park, C. R. Recent Advances in Hydrogen Storage Technologies Based on Nanoporous Carbon Materials. *Prog. Nat. Sci.: Mater. Int.* **2012**, *22*, 631−638.

(9) Murray, L. J.; Dincă, M.; Long, J. R. Hydrogen Storage in Metal-Organic Frameworks. *Chem. Soc. Rev.* **2009**, *38*, 1294−1314.

(10) Tylianakis, E.; Psofogiannakis, G. M.; Froudakis, G. E. Li-Doped Pillared Graphene Oxide: A Graphene-Based Nanostructured Material for Hydrogen Storage. *J. Phys. Chem. Lett.* **2010**, *1*, 2459−2464.

(11) Deshmukh, A.; Chiu, C.-c.; Chen, Y.-W.; Kuo, J.-L. Tunable Gravimetric and Volumetric Hydrogen Storage Capacities in Polyhedral Oligomeric Silsesquioxane Frameworks. *ACS Appl. Mater. Interfaces* **2016**, *8*, 25219−25228.

(12) Joseph, J.; Sivasankarapillai, V. S.; Nikazar, S.; Shanawaz, M. S.; Rahdar, A.; Lin, H.; Kyzas, G. Z. Borophene and Boron Fullerene Naterials in Hydrogen Storage: Opportunities and challenges. *ChemSusChem* **2020**, *13*, 3754−3765.

(13) Hashmi, A.; Farooq, M. U.; Khan, I.; Son, J.; Hong, J. Ultra-High Capacity Hydrogen Storage in a Li Decorated Two-Dimensional C_2N Layer. *J. Mater. Chem. A* **2017**, *5*, 2821−2828.

(14) Sunnardianto, G. K.; Bokas, G.; Hussein, A.; Walters, C.; Moultos, O. A.; Dey, P. Efficient Hydrogen Storage in Defective Graphene and its Mechanical Stability: A Combined Density Functional Theory and Molecular Dynamics Simulation Study. *Int. J. Hydrogen Energy* **2021**, *46*, 5485−5494.

(15) Khossossi, N.; Benhouria, Y.; Naqvi, S. R.; Panda, P. K.; Essaoudi, I.; Ainane, A.; Ahuja, R. Hydrogen Storage Characteristics of Li and Na Decorated 2D Boron Phosphide. *Sustainable Energy Fuels* **2020**, *4*, 4538−4546.

(16) Tan, X.; Tahini, H. A.; Smith, S. C. Conductive Boron-Doped Graphene as an Ideal Material for Electrocatalytically Switchable and High-Capacity Hydrogen Storage. *ACS Appl. Mater. Interfaces* **2016**, *8*, 32815−32822.

(17) Li, X.; Tan, X.; Xue, Q.; Smith, S. Charge-Controlled Switchable H_2 Storage on Conductive Borophene Nanosheet. *Int. J. Hydrogen Energy* **2019**, *44*, 20150−20157.

(18) Haldar, S.; Mukherjee, S.; Singh, C. V. Hydrogen Storage in Li, Na and Ca Decorated and Defective Borophene: a First Principles Study. *RSC Adv.* **2018**, *8*, 20748−20757.

(19) Li, L.; Zhang, H.; Cheng, X. The High Hydrogen Storage Capacities of Li-Decorated Borophene. *Comput. Mater. Sci.* **2017**, *137*, 119−124.

(20) Mannix, A. J.; Zhou, X.-F.; Kiraly, B.; Wood, J. D.; Alducin, D.; Myers, B. D.; Liu, X.; Fisher, B. L.; Santiago, U.; Guest, J. R.; Yacaman, M. J.; Ponce, A.; Oganov, A. R.; Hersam, M. C.; Guisinger, N. P. Synthesis of Borophenes: Anisotropic, Two-Dimensional Boron Polymorphs. *Science* **2015**, *350*, 1513−1516.

(21) Li, W.; Kong, L.; Chen, C.; Gou, J.; Sheng, S.; Zhang, W.; Li, H.; Chen, L.; Cheng, P.; Wu, K. Experimental Realization of Honeycomb Borophene. *Sci. Bull.* **2018**, *63*, 282−286.

(22) Kiraly, B.; Liu, X.; Wang, L.; Zhang, Z.; Mannix, A. J.; Fisher, B. L.; Yakobson, B. I.; Hersam, M. C.; Guisinger, N. P. Borophene Synthesis on Au(111). *ACS Nano* **2019**, *13*, 3816−3822.

(23) Er, S.; de Wijs, G. A.; Brocks, G. DFT Study of Planar Boron Sheets: A New Template for Hydrogen Storage. *J. Phys. Chem. C* **2009**, *113*, 18962−18967.

(24) Liu, Y.; Artyukhov, V. I.; Liu, M.; Harutyunyan, A. R.; Yakobson, B. I. Feasibility of Lithium Storage on Graphene and its Derivatives. *J. Phys. Chem. Lett.* **2013**, *4*, 1737−1742.

(25) Zhang, Y.; Cheng, X. Hydrogen Adsorption Property of Na-Decorated Boron Monolayer: A First Principles Investigation. *Physica E* **2019**, *107*, 170−176.

(26) Wang, J.; Du, Y.; Sun, L. Ca-Decorated Novel Boron Sheet: A Potential Hydrogen Storage Medium. *Int. J. Hydrogen Energy* **2016**, *41*, 5276−5283.

(27) Wen, T.; Xie, A.; Li, J.; Yang, Y. Novel Ti-Decorated Borophene $\chi 3$ as Potential High-Performance for Hydrogen Storage Medium. *Int. J. Hydrogen Energy* **2020**, *45*, 29059−29069.

(28) DOE Technical Targets for Onboard Hydrogen Storage for Light-Duty Vehicles. https://www.energy.gov/eere/fuelcells/doe-technical-targets-onboard-hydrogen-storage-light-duty-vehicles (accessed June 2021).

(29) Mannix, A. J.; Zhang, Z.; Guisinger, N. P.; Yakobson, B. I.; Hersam, M. C. Borophene as a Prototype for Synthetic 2D Materials Development. *Nat. Nanotechnol.* **2018**, *13*, 444−450.

(30) Li, Q.; Kolluru, V. S. C.; Rahn, M. S.; Schwenker, E.; Li, S.; Hennig, R. G.; Darancet, P.; Chan, M. K.; Hersam, M. C. Synthesis of Borophane Polymorphs Through Hydrogenation of Borophene. *Science* **2021**, *371*, 1143−1148.
(31) Mu, Y.; Li, S.-D. First-Principles Study on the Oxidation of Supported β12-Borophene. *J. Phys. Chem. C* **2020**, *124*, 28145−28151.
(32) Zhong, C.; Wu, W.; He, J.; Ding, G.; Liu, Y.; Li, D.; Yang, S. A.; Zhang, G. Two-Dimensional Honeycomb Borophene Oxide: Strong Anisotropy and Nodal Loop Transformation. *Nanoscale* **2019**, *11*, 2468−2475.
(33) Yan, L.; Liu, P.-F.; Li, H.; Tang, Y.; He, J.; Huang, X.; Wang, B.-T.; Zhou, L. Theoretical dissection of superconductivity in two-dimensional honeycomb borophene oxide B_2O crystal with a high stability. *npj Comput. Mater.* **2020**, *6*, No. 94.
(34) Zhang, R.; Li, Z.; Yang, J. Two-Dimensional Stoichiometric Boron Oxides as a Versatile Platform for Electronic Structure Engineering. *J. Phys. Chem. Lett.* **2017**, *8*, 4347−4353.
(35) Hu, J.; Zhong, C.; Wu, W.; Liu, N.; Liu, Y.; Yang, S. A.; Ouyang, C. 2D Honeycomb Borophene Oxide: a Promising Anode Material Offering Super High Capacity for Li/Na-ion Batteries. *J. Phys.: Condens. Matter* **2019**, *32*, No. 065001.
(36) Wang, Y.; Park, Y.; Qiu, L.; Mitchell, I.; Ding, F. Borophene with Large Holes. *J. Phys. Chem. Lett.* **2020**, *11*, 6235−6241.
(37) Penev, E. S.; Liu, Y.; Altalhi, T.; Kutana, A.; Yakobson, B. I. Stable Low-Dimensional Boron Chalcogenides from Planar Structural Motifs. *J. Phys. Chem. A* **2021**, *125*, 6059−6063.
(38) Kresse, G.; Furthmüller, J. Efficiency of Ab-Initio Total Energy Calculations for Metals and Semiconductors Using a Plane-Wave Basis Set. *Comput. Mater. Sci.* **1996**, *6*, 15−50.
(39) Kresse, G.; Furthmüller, J. Efficient Iterative Schemes for Ab-Initio Total-Energy Calculations Using a Plane-Wave Basis Set. *Phys. Rev. B* **1996**, *54*, No. 11169.
(40) Perdew, J. P.; Burke, K.; Ernzerhof, M. Generalized Gradient Approximation Made Simple. *Phys. Rev. Lett.* **1996**, *77*, No. 3865.
(41) Grimme, S. Semiempirical GGA-type Density Functional Constructed with a Long-Range Dispersion Correction. *J. Comput. Chem.* **2006**, *27*, 1787−1799.
(42) Chen, L.; Chen, X.; Duan, C.; Huang, Y.; Zhang, Q.; Xiao, B. Reversible Hydrogen Storage in Pristine and Li Decorated 2D Boron Hydride. *Phys. Chem. Chem. Phys.* **2018**, *20*, 30304−30311.
(43) Haldar, S.; Mukherjee, S.; Ahmed, F.; Singh, C. V. A First Principles Study of Hydrogen Storage in Lithium Decorated Defective Phosphorene. *Int. J. Hydrogen Energy* **2017**, *42*, 23018−23027.
(44) Liu, Z.; Liu, S.; Er, S. Hydrogen Storage Properties of Li-Decorated B2S Monolayers: A DFT Study. *Int. J. Hydrogen Energy* **2019**, *44*, 16803−16810.
(45) Varunaa, R.; Ravindran, P. Potential Hydrogen Storage Materials From Metal Decorated 2D-C 2 N: an Ab Initio Study. *Phys. Chem. Chem. Phys.* **2019**, *21*, 25311−25322.
(46) Chakraborty, B.; Ray, P.; Garg, N.; Banerjee, S. High Capacity Reversible Hydrogen Storage in Titanium Doped 2D Carbon Allotrope Ψ-Graphene: Density Functional Theory Investigations. *Int. J. Hydrogen Energy* **2021**, *46*, 4154−4167.
(47) Sathe, R. Y.; Dhilip Kumar, T. Electronic Structure Calculations of Reversible Hydrogen Storage in Nanoporous Ti Cluster Frameworks. *ACS Appl. Nano Mater.* **2020**, *3*, 5575−5582.
(48) Nosé, S. A Unified Formulation of the Constant Temperature Molecular Dynamics Methods. *J. Chem. Phys.* **1984**, *81*, 511−519.
(49) Hoover, W. G. Canonical Dynamics: Equilibrium Phase-Space Distributions. *Phys. Rev. A* **1985**, *31*, No. 1695.
(50) Verlet, L. Computer "Experiments" on Classical Fluids. I. Thermodynamical Properties of Lennard-Jones molecules. *Phys. Rev.* **1967**, *159*, No. 98.
(51) Momma, K.; Izumi, F. VESTA 3 for Three-Dimensional Visualization of Crystal, Volumetric and Morphology Data. *J. Appl. Crystallogr.* **2011**, *44*, 1272−1276.
(52) Chan, K. S.; Miller, M. A.; Peng, X. First-Principles Computational Study of Hydrogen Storage in Silicon Clathrates. *Mater. Res. Lett.* **2018**, *6*, 72−78.
(53) Bhatia, S. K.; Myers, A. L. Optimum Conditions for Adsorptive Storage. *Langmuir* **2006**, *22*, 1688−1700.
(54) Lee, H.; Choi, W. I.; Nguyen, M. C.; Cha, M.-H.; Moon, E.; Ihm, J. Ab Initio Study of Dihydrogen Binding in Metal-Decorated Polyacetylene for Hydrogen Storage. *Phys. Rev. B* **2007**, *76*, No. 195110.
(55) Wang, L.; Chen, X.; Du, H.; Yuan, Y.; Qu, H.; Zou, M. First-Principles Investigation on Hydrogen Storage Performance of Li, Na and K Decorated Borophene. *Appl. Surf. Sci.* **2018**, *427*, 1030−1037.
(56) Sandler, S. I. *An Introduction to Applied Statistical Thermodynamics*, 1st ed.; John Wiley & Sons: Hoboken, NJ, 2011.
(57) Kumar, S.; Dhilip Kumar, T. J. Electronic Structure Calculations of Hydrogen Storage in Lithium-Decorated Metal-Graphyne Framework. *ACS Appl. Mater. Interfaces* **2017**, *9*, 28659−28666.
(58) Lide, D. R. *CRC Handbook of Chemistry and Physics*, 75th ed.; CRC Press: New York, 1994.

https://doi.org/10.1021/acsami.1c09865
ACS Appl. Mater. Interfaces 2021, 13, 43233−43240